International Journal of Mineral Processing 138 (2015) 30–37

Contents lists available at ScienceDirect

International Journal of Mineral Processing

journal homepage: www.elsevier.com/locate/ijminpro

Zinc recovery during refractory ore biooxidation by an indigenous consortium

N. Marchevsky [a,b], M.S. Urbieta [a], C. Bernardelli [a], M. Mas [b], E.R. Donati [a,*]

[a] Centro de Investigación y Desarrollo en Fermentaciones Industriales (CINDEFI, CCT LA PLATA-CONICET, UNLP), Facultad de Ciencias Exactas, Universidad Nacional de La Plata, Calle 50 N° 227, 1900 La Plata, Argentina

[b] Departamento de Minería, Facultad de Ciencias Físico-Matemáticas y Naturales, Universidad Nacional de San Luis, San Luis, Argentina

ARTICLE INFO

Article history:
Received 1 February 2014
Received in revised form 12 November 2014
Accepted 13 March 2015
Available online 27 March 2015

Keywords:
Zinc bioleaching
Biooxidation
Gold recovery
Indigenous consortia

ABSTRACT

Two enrichment cultures (one iron oxidizing and one sulfur oxidizing) obtained from an acid mine drainage were physiologically and molecularly characterized; the first of them showed 99% 16S rRNA gene sequence similarity with *Leptospirillum ferrooxidans*, while the sulfur oxidizing species was highly related to *Acidithiobacillus ferrooxidans* and *Acidithiobacillus ferrivorans* sequences although, unlike them, the species in the enrichment culture does not seem to be able to oxidize iron. The consortium constituted by both enrichment cultures achieved a successful biooxidation of Hualilan ore allowing the increase of gold recovery up to 96.4% in the best culture condition (low pulp density in 1 K medium). At the same time, this condition showed an effective zinc bioleaching (up to 86%) although the recovery was much higher in cultures with initially supplemented iron; kinetics studies suggested that the bioleaching rate in 1 K medium at low pulp densities is controlled by diffusion through a layer mainly constituted by jarosite (rather than sulfur) which was detected in X-ray diffraction diagrams. The recovery of zinc as a subproduct of the pretreatment to optimize gold recovery would also allow the decrease of the metallic charge of the leachates from the biooxidation tanks which is an environmental advantage.

1. Introduction

In low grade refractory sulfide gold ore, gold is usually dispersed as microscopic particles within the pyrite and arsenopyrite matrices. Biooxidation is a well-known technology for the pretreatment of such ores that allows an efficient recovery of dispersed gold by the cyanidation method (Muravyov and Bulaev, 2013; Sun et al., 2012a, b). Mixed and pure cultures of acidophilic mesophiles and moderate and even extreme thermophiles have been used for the biooxidation of refractory gold ores; at high pulp densities (used in commercial applications) mesophiles showed better biooxidation potential compared to moderate and extreme thermophiles (Ciftci and Akcil, 2010). Even when there are some contradictory results in the literature, indigenous microbial communities usually seem to be superior to microbial consortia constructed using strains from other environments (Bryan et al., 2011; Chandraprabha et al., 2002).

During biooxidation processes, other valuable metals can be released to the solutions by microbial action (Dinkla et al., 2013; Kaewkannetra et al., 2009; Kondrat'eva et al., 2012). The recovery of such metals as subproducts of the main process would allow not only an economical advantage but also an environmental improvement, decreasing the metallic charge of the leachates from the biooxidation tanks. Recovery of zinc is still performed using conventional methods (pyrometallurgical smelting of concentrates) with bioleaching being only used at pilot scale (see below) but this procedure excludes low-grade or refractory ores. For these ores, heap bioleaching (and consequently a slower process) instead of tank bioleaching should be performed to avoid intensive grinding which would make the process uneconomical. Biooxidation is operated in stirred tanks for high-grade ores or gold concentrates; in this way high reaction rates are obtained and the capital and operating costs are justified by gold market price. The solubilization of zinc during the biooxidation process might imply that the recovery of this metal could be achieved using a less contaminating technology and without any additional investment. After biooxidation, residues might be leached by cyanidation and the solutions might be used in downstream processing for zinc recovery.

Hualilan area is considered one of the most important sources of gold in San Juan Province (Argentina) in the Southern Andes. The earliest recorded mining activity in the area predates the Spanish conquest and it intensified after. The chemical composition of the ore – although highly variable – reveals an average content of 10 ppm Au – partially refractory – 80 ppm Ag and up to 8% Zn mainly as sphalerite. Sphalerite is one of the most important sources for Zn production in the world. Zn

* Corresponding author.
E-mail address: donati@quimica.unlp.edu.ar (E.R. Donati).

http://dx.doi.org/10.1016/j.minpro.2015.03.009
0301-7516/

extraction from sphalerite using bioleaching has recently attracted more attention due to the economic and ecological advantages of this technology over traditional roasting and smelting (Deveci et al., 2004; Giaveno et al., 2007; Haghshenas et al., 2009; Mousavi et al., 2007; Rodriguez et al., 2003; Shi et al., 2006; Soleimani et al., 2011; Souza et al., 2007).

The aim of this investigation is to study the recovery of zinc during biooxidation of a refractory gold-bearing ore from Hualilan district. Enrichment cultures containing sulfur and iron oxidizing bacteria were obtained from different samples taken from an acid mine drainage. An artificial consortium mixing these enrichment cultures was used as inoculum in biooxidation experiments after characterization of both cultures by fluorescence in situ hybridization and 16S rRNA gene cloning and sequencing. In biooxidation experiments, additions of different alternative energy sources, different initial pH values and pulp densities were tested in order to find suitable conditions for recovering both metals.

2. Materials and methods

2.1. Mineral

Mineral samples from Hualilan mining area (San Juan province, Argentina) were used throughout this study. The main mineralogical components were pyrite, pyrrhotite, galena, sphalerite, and chalcopyrite. Besides, limestone and dolomitic limestone were detected in the sample. The chemical composition of the sample was 25.67 g/t Au, 190.2 g/t Ag, 11.53% Fe, 8.12% Zn, 1.3% Mn, and minor amounts of other metals (476 g/t Cd, 1403 g/t Cu, 698 g/t Pb). The fraction with size particle less than 74 μm was used in the biooxidation experiments.

2.2. Microorganisms and media

Several water and sediment samples were taken from the acid mine drainage near to La Carolina mining (San Luis province, Argentina). Environmental samples were directly inoculated in 9 K medium or in the same medium without iron (0 K) supplemented by elemental sulfur powder 10 $g \cdot L^{-1}$. The pH values were initially adjusted to 3 for 0 K medium and 1.8 for 9 K medium utilizing H_2SO_4 (1:10). Media with basal salts were sterilized by autoclaving (20 min at 121 °C and 1 atmosphere overpressure), while solution containing iron was sterilized by filtration through a 0.2 μm pore size filter. The enrichment cultures were made in Erlenmeyer flasks containing 100 mL final volume and inoculated at 10% (v/v) or 2 g for water samples and sediments respectively. The flasks were incubated at 30 °C and agitated at 150 rpm in an orbital shaker. Enrichment cultures that showed microorganism growth were maintained by successive transfer in respective medium at the same conditions. Ferrous iron oxidation and sulfur oxidation rates were evaluated for all the enrichment cultures. The two most efficient were selected to perform the biooxidation experiments. Iron(II) and sulfur oxidizing cultures were called LC-1 and LC-2 respectively and they were unable to oxidize the other energy source.

2.3. Fluorescence in situ hybridization (FISH)

Aliquots of 1 mL of active cultures of LC-1 and LC-2 were used for fluorescent in situ hybridization (FISH) assays. Samples were fixed with paraformaldehyde at 4% final concentration for 4 h at 4 °C and then filtered through GTTP 0.25 Millipore membranes (0.22 μm) using a filtration column. Filters were washed and neutralized with 20 mL of PBS buffer (130 mM NaCl, 7 mM Na_2HPO_4, 3 mM NaH_2PO_4, pH 7.2) and air dried. Hybridizations were done following Amann's protocol (Amann, 1995) using Cy3 labeled probes: TF539 (5′ CAG ACC TAA CGT ACC GCC 3′, 20% formamide in hybridization buffer) specific for *Acidithiobacillus ferrooxidans*, ATT223 (5′ AGA CGT AGG CTC CTC TTC 3′, 40% formamide in hybridization buffer) specific for *Acidithiobacillus thiooxidans* and LF665 (5′ CGC TTC CCT CTC CCA GCC T 3′, 35% formamide in hybridization buffer) specific for *Leptospirillum ferrooxidans*. 4′,6′-Diamidino-2-phenylindole (DAPI) stain was used in all hybridizations to evaluate total cell number. Dako Fluorescent Mounting Medium (Dako North America Inc., USA) was added to preparations in order to avoid fluorescence fading. A Leica DM 2500 epifluorescence microscope was used to visualize hybridization results. Images were taken using a Leica DFC 300 FX camera and its corresponding software (Leica Microscopy Systems Ltd, Heerbrugg, Switzerland).

2.4. DNA extraction, 16S rRNA gene cloning and sequencing comparison

Two microliters of each enrichment culture was filtered to retain solid residues and centrifuged 15 min at 13,000 rpm. Cell pellets were washed with pH 1.5 (H_2SO_4) water, resuspended in 1 mL TE buffer (10 mM Tris HCl pH 8.0, 1.0 mM EDTA). Cells were incubated with 250 μL of 10% sucrose in TE buffer and 250 μL of 5 μg/mL lizosime in TE buffer solution at 37 °C for 1 h. To improve cell lysis 100 μL of solution of protease K 5 mg/mL and SDS 10% in TE buffer were added and incubated 1 h at 37 °C. In order to separate aqueous and organic phases 70 μL sodium acetate 3.0 M (pH 3.4), 100 μL of chloroform and 200 μL phenol–Tris were added and centrifuged 15 min at 13,500 rpm. Aqueous phase was extracted using 100 μL of chloroform and centrifuged 15 min at 13,500 rpm for decanting cellular rests. Cold isopropyl alcohol was used for DNA precipitation in 1 h incubation at −20 °C and 20 minute centrifugation at 13,500 rpm using a refrigerated (4 °C) centrifuge. DNA pellet was washed with 70% cold ethanol and air dried. DNA was resuspended in 50 μL of TE buffer and incubated at 60 °C for 1 h.

Bacteria general primers 27F: 5′-AGAGTTTGATCCTGGCTCAG -3′ and 1541: 5′-AAGGAGGTGATCCAGCCGCA-3′ were used for amplifying DNA extracted from enrichment cultures (Achenbach and Woese, 1995). PCR conditions were as follows: initial denaturation at 95 °C for 5 min, followed by 38 cycles of denaturation at 95 °C for 1 min, annealing at 48 °C for 1 min and extension at 72 °C for 1 min and a final step of extension at 72 °C for 10 min. Amplification reactions contained 3 μL of DNA solution per 25 mL reaction volume, 1× PCR buffer (Promega Biotech), 2.5 mM of each of the deoxynucleotides, 2.5 mM $MgCl_2$, 500 mM of the forward and reverse primers and 0.025 $U \cdot mL^{-1}$ of Taq DNA polymerase (Promega Biotech). PCR amplification was checked by 1.5% agarosa gel electrophoresis stained with ethidium bromide.

Amplified 16S rRNA gene products (>1400 bp) were cloned using the Topo Ta Cloning Kit (Invitrogen. CA, USA) and sequenced using Macrogen services (Macrogen Inc., Seul Korea).

16S rRNA gene sequences of LC-1 and LC-2 enrichment cultures were checked for potential chimeras using Bellerophon Chimera Check program (http://greengenes.lbl.gov/cgi-bin/nph-bel3_interface.cgi) and Maillard software. Finally they were compared with NCBI database using BLAST (http://ncbi.nlm.nih.gov/BLAST). LC-1 and LC-2 16S rRNA sequences, together with their closest relatives were aligned using ARB package (http://www.arb-home.de). Alignments were corrected manually and phylogenetic trees were constructed using neighbor-joining (Saitou and Nei, 1987) and Jukes–Cantor correction. The robustness of individual branches was estimated by bootstrapping with 1000 replicates (Felsenstein, 1985).

2.5. Biooxidation experiments

Leaching experiments were conducted in 250 mL Erlenmeyer flasks containing 150 mL of 0 K medium at 2% of pulp density. H_2SO_4 0.5 M was added to adjust the initial pH value at 1.8. The inoculum was composed of a mixed culture of LC-1 and LC-2. LC-1 was previously cultivated in 9 K medium (pH 1.8) and LC-2 in 0 K medium with elemental powder sulfur at 0.67% (w/v). After bacterial growth reached exponential phase, cultures were filtered through blue ribbon filter paper to eliminate iron precipitates or sulfur. Cells were harvested by centrifugation, resuspended in basal salt

medium without energy sources and then mixed to form the inoculum containing approximately 5×10^8 cell·mL^{-1}.

Biooxidation experiments were carried out in varying energy sources, initial pH values and pulp densities. In the first case, iron(II) (1 g·L^{-1}–1 K medium) and/or sulfur powder (0.67% w/v) were used in systems with mineral at 2% (w/v) pulp density and initial pH values of 1.8. In the second case, initial pH values were 1.5, 1.8, and 2.2; these experiments were done in 1 K medium and 2% (w/v) pulp density. Finally, to consider the effect of pulp density the experiments were done in 1 K medium at initial pH of 1.8. The pulp densities used were 1%, 5% and 10%. Table 1 summarizes the systems carried out in the experiments.

Bioleaching was performed by duplicate and abiotic controls were made replacing the inoculum by fresh media. The flasks were incubated at 150 rpm and 30 °C. Three microliters of samples was routinely drawn from the flasks to analyze iron, zinc, Eh, pH and bacterial population. Before taking the sample for analysis, the volume of the Erlenmeyer flasks was adjusted with sterilized water.

2.6. Analytical determination

Eh and pH were measured with specific electrodes. Iron(II) and proton concentrations in the enrichments were determined by titration with $KMnO_4$ or NaOH, respectively. These parameters were used to follow the bacterial growth. At the same time, bacterial population in the liquid phase was determinate by direct counting in a Petroff-Hausser chamber using a phase-contrasting microscope. In samples from leaching experiments, iron(II) was determined by the colorimetric ortho-phenanthroline method, modified as follows: 0.1–0.3 mL of sample (or its dilution), 1.4–1.2 mL of HCl 1:20, 0.5 mL of ammonium acetate buffer and 0.5 mL of o-phenanthroline (1 g/L). Zn and total soluble Fe concentrations were determined by an atomic absorption spectrophotometer (AAS) after appropriate dilution in HNO_3 0.14 N.

Solid residues from biooxidation experiments were used for cyanide leach process. Leaching was carried out at 25% mineral pulp density in 1.5 g·L^{-1} of sodium cyanide solution; lime was added to keep the pH of the solution at about 10.5–11.0. After 48 h of leaching with natural air supply at room temperature, the gold bearing liquid was separated from the solids and the tailings are washed to remove gold and cyanide. Gold concentration was measured using atomic absorption spectrophotometry after extraction from an aqueous cyanide solution using di-isobutyl ketone (DIBK).

3. Results and discussion

3.1. Physiological and phylogenetic analysis of LC-1 and LC-2 enrichment cultures

Fig. 1a shows that the LC-1 culture is oxidizing ferrous to ferric iron. Cells grown in soluble ferrous iron were mostly curved rod shaped, similar to bacteria from the genus *Leptospirillum*. This enrichment culture showed one of the fastest ferrous iron oxidation rates in comparison with the others obtained from the samples studied that also had an iron oxidizing activity. LC-1 culture showed a lag phase of about 12 hs and after that ferrous iron oxidation rapidly increased. When ferrous iron was exhausted, Eh and pH reached the final values of 600 mV and 2.3 respectively. The specific growth rate constant (μ) was calculated to be 0.0576 h^{-1} which is lower than those usually reported for *A. ferrooxidans* (Nemati et al., 1998; Li et al., 2013) but similar to those *for L. ferrooxidans* (Breed et al., 1999) under similar conditions (batch cultures in similar pH and T conditions).

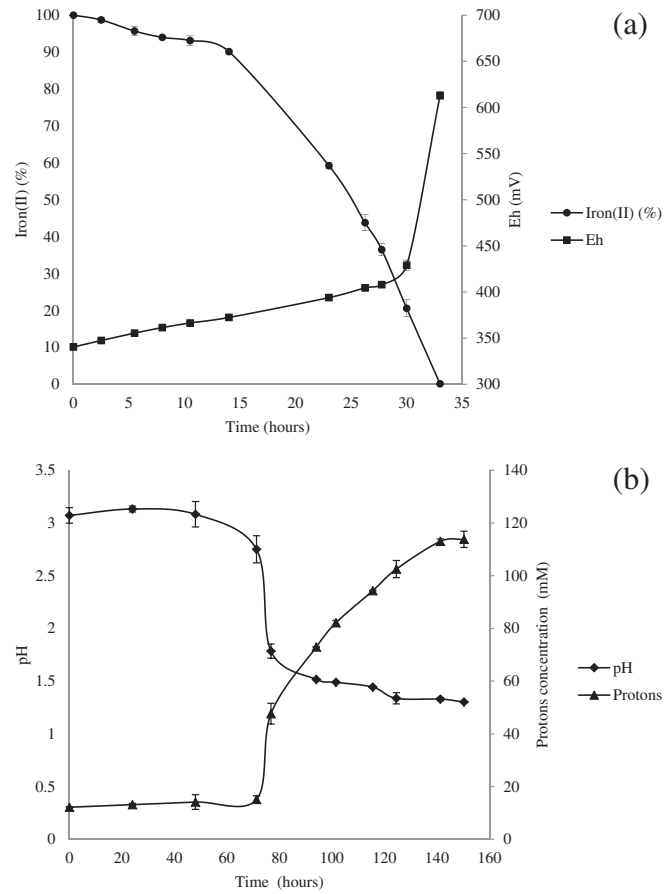

Fig. 1. Microbial growth (a) LC-1 on ferrous iron; (b) LC-2 on elemental sulfur. Figure is *.xlsx file (Microsoft Office Excel); the figure was later pasted in a Microsoft Office Word file.

LC-2 enrichment culture derived energy from the autotrophic oxidation of elemental sulfur (see Fig. 1b) but it was unable to grow in cultures with ferrous iron as the only energy source after 25 days (data not shown). Cells were motile rods, similar to those expected for *Acidithiobacillus* genus. When grown on sulfur, the culture showed a long lag phase (about 3 days) and then there was a fast increase in acid production and pH decrease (Fig. 1b). A final pH value of 1.3 was reached after 6 days. The specific growth rate constant was calculated to be 0.0112 h^{-1} which is lower than those obtained for *Acidithiobacillus* cultures under similar conditions (Ceskova et al., 2002; Espejo and Romero, 1987; Kupka et al., 2003).

Hybridization with probe LF665 (specific for *L. ferrooxidans*) was positive for most of cells present in LC-1 culture. Cells from LC-2 culture showed positive hybridization with THIO1 probe (specific for *Acidithiobacillus* genus) and also with TF539 probe (specific for *A. ferrooxidans*); and showed no hybridization with ATT223 probe specific for *A. thiooxidans*. Fig. 2 shows epifluorescence microscope

Table 1
Conditions of biooxidation experiments.

System	Pulp density	1 g·L^{-1} Fe(II)	6.7 g·L^{-1} sulfur	Initial pH value
1	1	X	–	1.8
2	2	X	–	1.5
3	2	X	–	1.8
4	2	X	–	2.2
5	2	X	X	1.8
6	2	–	–	1.8
7	2	–	X	1.8
8	5	X	–	1.8
9	10	X	–	1.8

´X´ means that this particular condition was used (´-´ means the opposite).

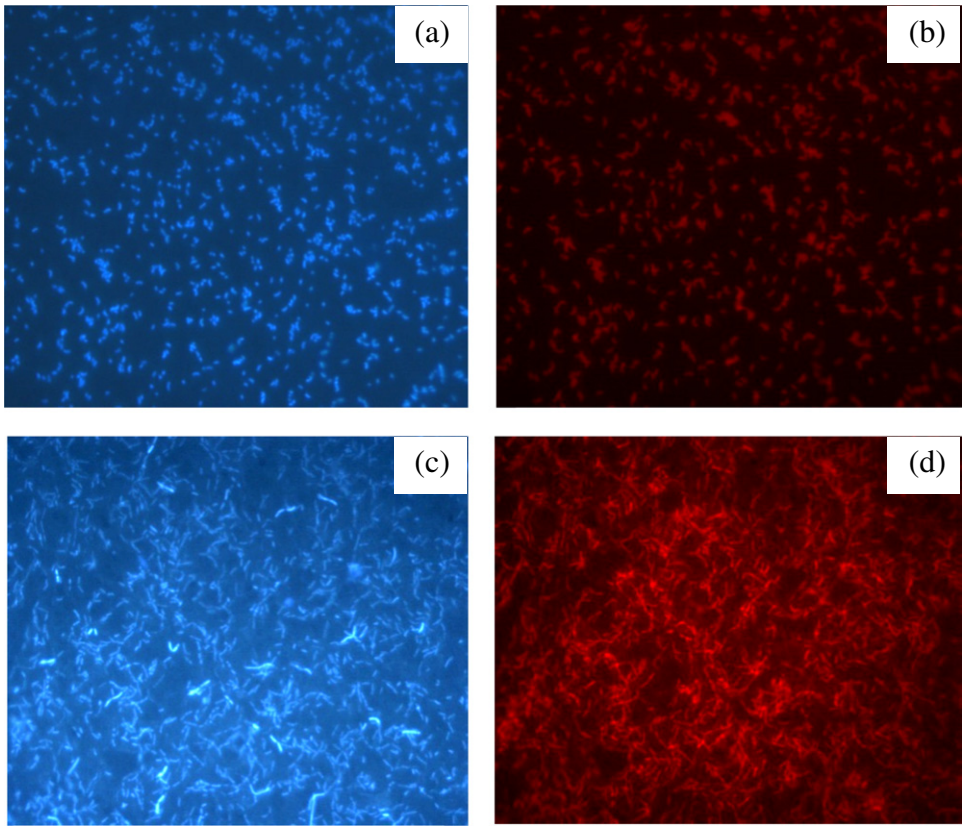

Fig. 2. Epifluorescence microscope images of LC-1 cells stained with DAPI (a) and LF665 probe specific for *L. ferrooxidans* (b); LC-2 cells stained with DAPI (c) and TF539 probe specific for *A. ferrooxidans* (d).
Figures are *.jpg files and were later pasted in a Microsoft Office Word file.

images of both consortia stained with DAPI (left) or with specific probes (right). As it is well known, *A. ferrooxidans* oxidize not only reduced sulfur compounds but also ferrous iron. However as it was indicated above that the LC-2 culture did not show any ferrous iron oxidation even after 3 weeks (data not shown).

Phylogenetic associations of 16S rRNA gene sequences from LC-1 and LC-2 cultures are shown on phylogenetic trees in Fig. 3 (a and b, respectively). According to BLAST comparison, LC-1 16S rRNA gene sequence shows 99% similitude with many *L. ferrooxidans* sequences. LC-2 16S rRNA gene sequence presents similarities of 98–99% to different sequences of *Acidithiobacillus ferrivorans* and *A. ferrooxidans*. As it can be seen in Fig. 3b, LC-2 sequences are more closely related to *A. ferrivorans* group, a particular one among *A. ferrooxidans* cluster. It is worth mentioning that the target sequences of TF539 probe are present in both *A. ferrooxidans* and *A. ferrivorans* 16S rRNA gene sequences.

According to this analysis LC-2 bacteria are closely related to iron- and sulfur-oxidizing species such as *A. ferrooxidans* and *A. ferrivorans*, however they proved to be unable to oxidize iron under the conditions assayed. Zhang et al. (2013) reported a strain which also presents an unusual behavior; cells coming from cultures growing on elemental sulfur were unable to oxidize ferrous iron. However, the results reported by Zhang and collaborators could be explained due to the high acidity of the biomass coming from a culture grown on elemental sulfur (Curutchet and Donati, 2000). Future studies need to be done in order to clarify whether LC-2 is a strain of known iron and sulfur-oxidizers (*A. ferrooxidans* or *A. ferrivorans*) with an unusual physiological characteristic that does not allow ferrous iron oxidation under the assayed conditions or if it is a novel only sulfur-oxidizing species phylogenetically related to *A. ferrooxidans* and *A. ferrivorans*.

3.2. Biooxidation experiments

Experiments were monitored until their metal (Fe, Zn) concentrations in solution reached a steady state: about 30 days at low pulp densities and 50 days for the high pulp densities.

Fig. 4 shows the evolution of pH values in cultures and sterile controls in the different series of experiments varying pulp densities, initial pH values and energy sources.

In sterile controls pH increased due to the presence of certain amounts of carbonates and limestone whose dissolution generated acid consumption. The maximum pH values (3.2–3.4) were reached in sterile controls at high pulp density. In inoculated systems a rapid increase in pH values was observed in the first 5–10 days (depending on the pulp density) probably due to the dissolution of different species from the ores and the iron biooxidation which also consumes acid. Eq. (1) shows the process catalyzed by iron oxidizing microorganisms (present in LC-1 enrichment culture which was part of the inoculum). Similar behavior was observed in all cultures including those at different initial pH values although at the lowest initial pH (1.5) the increase was not so significant.

$$4\,Fe^{2+} + 4\,H^{+} + O_2 \rightarrow 4\,Fe^{3+} + 2\,H_2O \quad (1)$$

After the first increase in pH, a progressive decrease to reach values close to 1.4–1.5 was observed (Fig. 4). Different processes could have contributed to this behavior: acid produced by the oxidation of certain sulfides like pyrite, ferric iron hydrolysis plus microbial oxidation of elemental sulfur which could have been formed during sulfides oxidation. These well-known processes are shown in Eqs. (2)–(4). Although several ferric iron precipitates (jarosite,

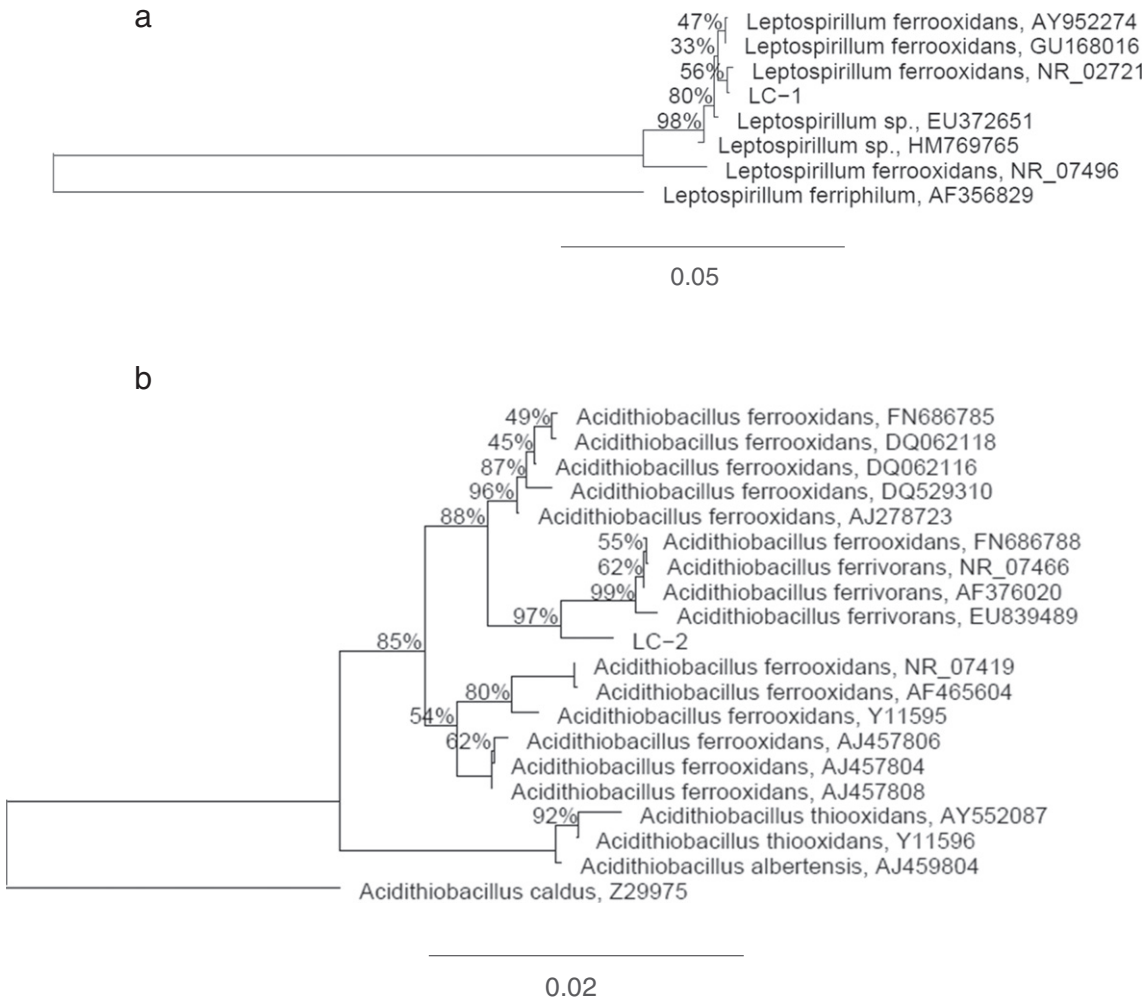

Fig. 3. Phylogenetic trees from 16S rRNA gene sequences of LC-1 (a) and LC-2 (b). The numbers at the branch nodes are percentage bootstrap values based on 1000 replications. The scale bar represents the number of fixed mutations per nucleotide positions.
Figures are *.pptx files (Microsoft Office Power Point) and were later pasted in a Microsoft Office Word file.

goethite, hematite, schwertmannite, and ferrihydrite) can be formed, Eq. (4) shows ferric iron hydrolysis only to form jarosite as it is the most stable insoluble phase under the culture conditions (pH less than 2, redox potential higher than 563 mV vs. Ag/AgCl). In cultures where elemental sulfur was supplemented, lower pH values (close to 1.2) were achieved because process represented by Eq. (3) is favored.

$$FeS_2 + 14\,Fe^{3+} + 8\,H_2O \rightarrow 15\,Fe^{2+} + 16\,H^+ + 2\,SO_4{}^{2-} \quad (2)$$

$$S_8 + 12\,O_2 + 8\,H_2O \rightarrow 8\,SO_4{}^{2-} + 16\,H^+ \quad (3)$$

$$3\,Fe^{3+} + 2\,SO_4{}^{2-} + 6\,H_2O + K^+ \rightarrow KFe_3(SO_4)_2(OH)_6 + 6\,H^+ \quad (4)$$

Fig. 5 shows percentages of zinc solubilization for the different experimental conditions assayed after 28 days. In graph (a) a typical kinetics of zinc solubilization obtained in the experiments at two different pulp densities is also shown.

At low pulp densities and almost independently of the other culture conditions, maximum dissolution was achieved in few days (about 5–7 days) while at higher pulp densities 20–30 days were needed to reach maximum extraction. At the end of the experiments all the cultures reached extractions higher than 80% at low pulp densities; the effect of the addition of other energy sources or the decrease in pH did not produce any significant change. Increasing pulp density decreased zinc recovery, which was 70% for the highest pulp density used (10% w/v).

Sterile controls showed zinc extractions lower than 30%, except in the lowest initial pH value (1.5); this fact demonstrates that the dissolution of sphalerite is partially supported by acid attack. In inoculated flasks an additional process to mere acid attack is operating, as it is suggested by higher zinc dissolutions than in sterile controls even with similar pH values at the end of the experiments. As it is widely accepted, sphalerite can be degraded by acidophilic autotrophic bacteria through the polysulfide pathway. The process can be represented as follows:

$$ZnS + Fe^{3+} + H^+ \rightarrow Zn^{2+} + 0.5\,H_2S_n + Fe^{2+} (n \geq 2) \quad (5)$$

$$0.5\,H_2S_n + Fe^{3+} \rightarrow 0.125\,S_8 + Fe^{2+} + H^+. \quad (6)$$

Ferrous iron produced in reactions (5) and (6) can be reoxidized to ferric ion by iron oxidizing microorganisms while elemental sulfur formed in the last reaction can be oxidized according to Eq. (3).

When comparing zinc extractions from inoculated systems supplemented with ferrous iron and/or sulfur, it seems that both additions caused a significant, although not dramatic decrease in zinc solubilization. The culture without any supplement (number 6) achieved the maximum zinc extraction (almost 95%). This

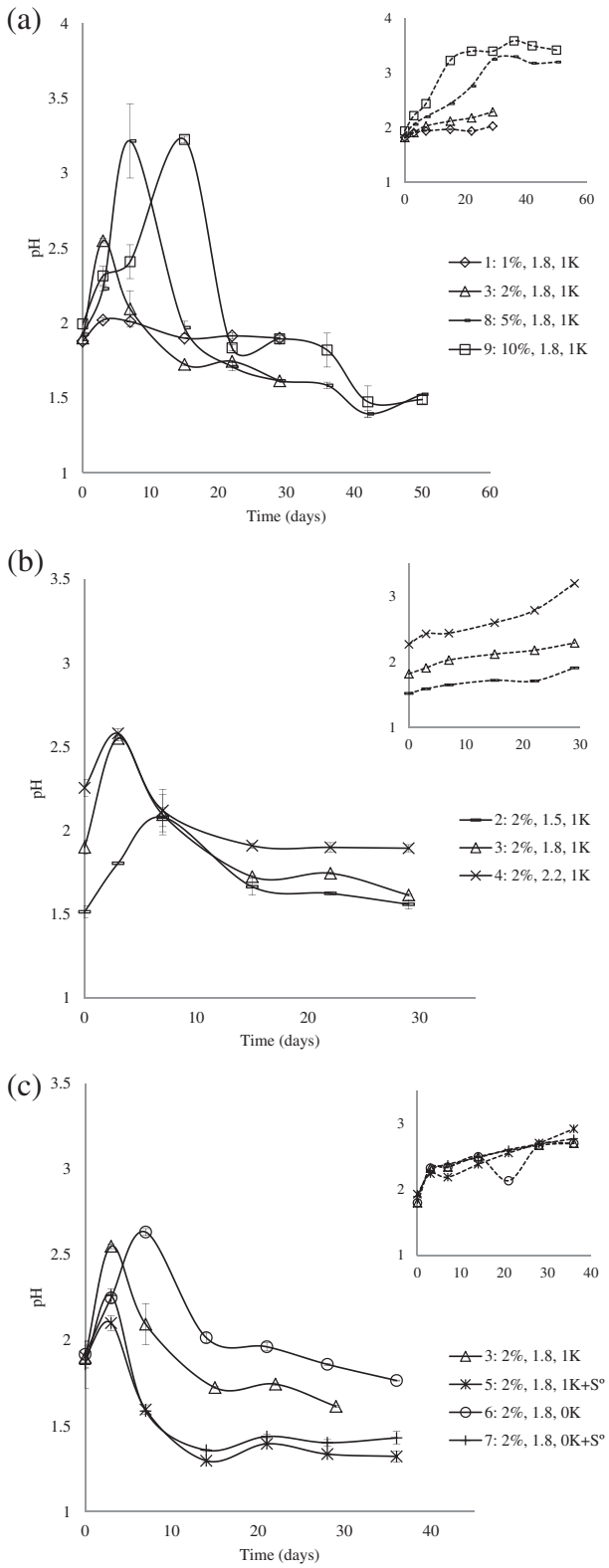

Fig. 4. Evolution of pH values during biooxidation experiments in cultures with different: (a) pulp densities (b) initial pH values and (c) energy sources. The inner graphs show the behavior of the corresponding sterile.
Figures are *.xlsx files (Microsoft Office Excel) and were later pasted in a Microsoft Office Word file.

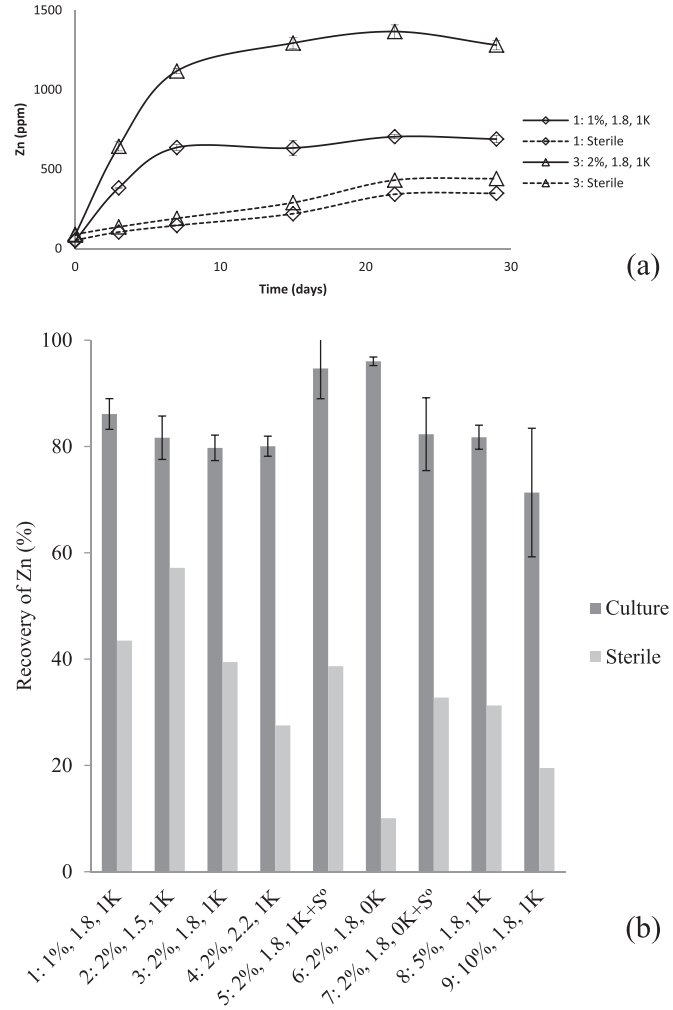

Fig. 5. (a) Typical kinetics of zinc solubilization; (b) percentages of zinc dissolution after 28 days.
Figures are *.xlsx files (Microsoft Office Excel) and were later pasted in a Microsoft Office Word file.

behavior can be explained by the increase of jarosite precipitation in cultures with supplemented iron. The layer of jarosite can cover the mineral slowing, reducing or even avoiding sulfide dissolution (see Section 3.3). This was confirmed by X-ray diffraction where jarosite peaks are increased in the residues coming from assays done in 1 K medium.

On the other hand, the addition of sulfur caused a decrease in zinc solubilization because sulfur offersoffers an additional surface for microbial attachment and that decreases the number of cells able to attach and to leach the sulfide (through the contact mechanism). In the same way, sulfur oxidizing microorganisms can use the supplemented sulfur as energy source instead of the sulfur – formed according to Eq. (6) – which covers the mineral surface and reduces the sulfide dissolution.

Fig. 6 shows iron concentration in cultures and abiotic controls at the end of the experiments. In this ore, gold is dispersed mostly within the pyrite matrix. In previous studies (data not shown) we proved that the extent of biooxidation is mainly determined by the amount of solubilized iron as it has been also reported (Mousavi et al., 2007). Surely, this is because pyrite is an acid-insoluble metal sulfide which needs an oxidation process (in this case mediated by ferric iron coming from the microbial catalysis of ferrous iron oxidation represented in Eq. (1)) to be dissolved. That is the reason why in abiotic controls (without any continuous re-oxidation of ferrous iron) iron solubilization was lower (less than 30%). In cultures where iron was initially supplemented and especially in those with high initial pH values, iron precipitation was abundant and the final soluble concentration was lower than the

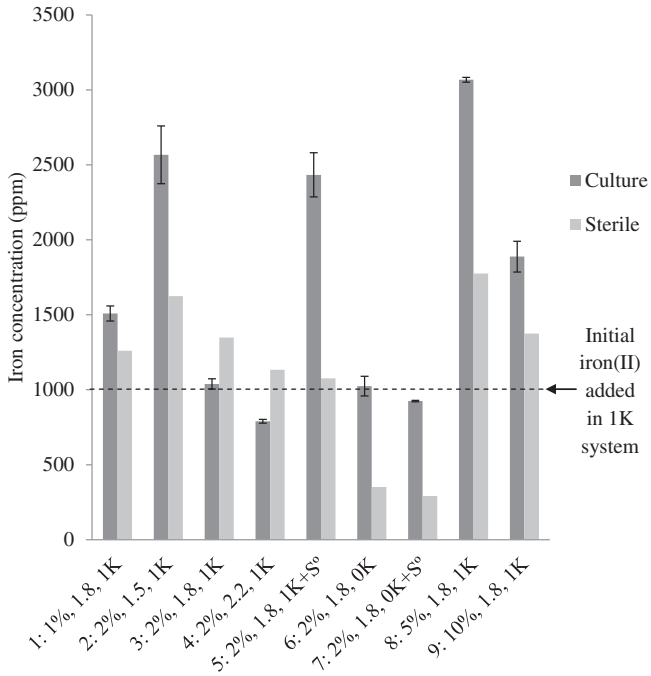

Fig. 6. Total soluble iron concentrations after 28 days.
Figure is *.xlsx file (Microsoft Office Excel) and was later pasted in a Microsoft Office Word file.

initial. Jarosite precipitation surely limited the transfer of oxygen and/or ferric iron ions to fresh sulfide mineral. In any case, the effect of iron precipitates on iron solubilization was significantly higher than on zinc recovery.

At 28 days, the highest iron solubilization (more than 90%) was detected in the culture with the lowest pulp density in 1 K medium. A negative effect on iron dissolution was visualized with the increase on pulp density. Although the addition of sulfur allowed reaching lower pH values iron solubilization was not enhanced.

3.3. Cyanide leaching and gold recovery

Similar biooxidation assays but using higher volumes (1000 mL) in 1 K medium and 10% w/v pulp density were carried out under identical conditions. 94.2% iron and 74.0% zinc were extracted after 82 days when a steady state was reached. Residues from these cultures and from the corresponding abiotic control were subjected to cyanide leaching. Gold recoveries were 96.4 and 75.0% for the residues obtained in biooxidation assays and in abiotic controls respectively. It means that biooxidation pre-treatment allowed a 30% increase in gold recovery with a cyanide consumption of 15% lower than that observed for the residue from abiotic control. The last result is in contradiction to that usually reported indicating that although the biooxidation pre-treatment achieves better gold recoveries, the cyanide consumption is moderately increased (Ciftci and Akcil, 2010).

These results show the efficiency of biooxidation (biological oxidation) to liberate the originally refractory gold from sulfidic matrix allowing later attack by cyanide leaching. Although these experiments were carried out under a condition of pulp density lower than those usually used at commercial scale (15–20% w/v), the results suggest that the biooxidation treatment was successful and higher gold recovery could be achieved supplementing the leaching medium with a small concentration of ferrous iron. At the same time, although cultures supplemented with ferrous iron and high pulp density did not achieve maximum zinc recovery, zinc dissolution was significantly enhanced and zinc could be recovered from the leachates after the biooxidation process.

3.4. Kinetic analysis of zinc bioleaching

Dissolution of metals from sulfide ores has been mainly explained by the shrinking core model (Brochot et al., 2004; da Silva, 2004; Fowler and Crundwell, 1999; Ghorbani et al., 2013; Safari et al., 2003). The reaction rate in solid–liquid heterogeneous systems (such as bioleaching) is controlled by any of the sequential steps that occur in the solid–liquid interface: diffusion through the liquid film, diffusion through the product layer and chemical reaction (Kodali et al., 2004; Levenspiel, 1972). If bioleaching experiments are carried out in shaking condition, it can be assumed that bioleaching rates are not limited by diffusion through the liquid film (Mishra et al., 2008), and the process can be evaluated preferably according to the other two stages.

Previous works on kinetics of sphalerite bioleaching by mesophilic bacteria suggested that diffusion through the product layer is the rate-controlling mechanism (da Silva, 2004; Giaveno et al., 2007; Liao and Deng, 2004; Lizama, 2004). During bioleaching, elemental sulfur (due to the oxidation of sulfide by iron(III)) and/or iron precipitates (mainly jarosite but probably also other ferric iron compounds such as goethite, hematite, schwertmannite, and ferrihydrite) are formed as insoluble products. It is known that these precipitates generate a layer over the reactant surface and increase the path length for diffusion. If bioleaching kinetic is controlled by diffusion through these product layers, the kinetics would be fitted by using Eq. (7):

$$K_p.t = 1-(2/3).X-(1-X)^{2/3} \quad (7)$$

where, K_p = parabolic rate constant (day^{-1}); t = time (d); and X = fraction reacted of zinc.

On the other hand, Gomez et al. (1999) established that the chemical reaction is the controlling step of the bioleaching process, even though the formation of a product layer as a result of jarosite precipitation and sulfur generation was also observed. When the process is controlled by chemical reaction, Eq. (8) must be used.

$$K_p.t = 1-(1-X)^{1/3} \quad (8)$$

Using the experimental zinc bioleaching data presented here, plots of $(1-2/3X-(1-X)^{2/3})$ versus time and $(1-(1-X)^{1/3})$ versus time were constructed. Linear fits were done using all experimental values. The colonization period of the ore reported by Lizama (2004) was not observed.

When considering the effect of initial pH, the model of zinc dissolution kinetic controlled by diffusion through the product layer correlates much better than the one of kinetic limited by chemical reaction, as the correlation coefficients were 0.97 and 0.93 respectively for an initial pH value of 1.8 and 0.97 and 0.94 for an initial pH value of 2.2. For the lowest initial pH value (1.5) the regression coefficients were very similar (around 0.98) indicating that neither diffusion nor chemical reaction was dominant on zinc dissolution kinetic. Since jarosite, neither sulfur nor other ferric iron phase, was detected in X-ray diffraction analysis, we assumed that jarosite constitutes the layer limiting the rate of bioleaching, in agreement with our prior suggestion in Section 3.2. This is also supported by the presence of sulfur oxidizing microorganisms that continually consume the sulfur layer. In addition, lower pH values would diminish the massive jarosite precipitation (although not completely as pH increases at the beginning of the bioleaching process) justifying why the limitation by this layer is not so important at initial pH 1.5.

The kinetic model fits obtained for different pulp densities were directly associated with the contents of mineral present in the system. At low pulp density (1% and 2%) better linear fits were obtained for the model of diffusion through the product layer as the limiting step

(0.97 against 0.93), while systems with higher pulp density values (5% and 10%) showed better fits for kinetic limitation by the chemical reaction model (0.96 against 0.90). This might be related to the increase of the exposed surface of the mineral at high pulp densities. In this way, at low pulp densities the surface is completely covered by jarosite making the kinetic limitation by the diffusion process dominant over the limitation by chemical reaction. At high pulp densities (equal or higher than 5%), the products (precipitates) formed during bioleaching would not cover the surface completely, leaving chemical reaction as the limiting step. This is in agreement with previous reports (Acevedo et al., 2004). In addition, the use of high pulp densities has other effects in the process like attrition of microorganisms by the mineral particles, and decrease in oxygen transfer. All these factors diminish microbial activity affecting zinc dissolution (Deveci et al., 2004; Fowler and Crundwell, 1999; Mousavi et al., 2007) although these effects are usually significant at pulp densities higher than 15%.

Finally, the analysis of the two kinetic models showed no significant differences with the energy sources used to supplement the inoculum (ferrous iron or sulfur), indicating that the kinetic control of this bioleaching process is mostly related to pulp density and assays initial pH values.

4. Conclusions

A consortium composed of two enrichment cultures (one iron oxidizing and one sulfur oxidizing) achieved a successful biooxidation of Hualilan ore allowing the increase of gold recovery up to 96.4% in the best culture condition (low pulp density in 1 K medium) with a lower cyanide consumption. During biooxidation process, up to 86% of zinc was solubilized through a process whose kinetics was controlled by diffusion through a layer mainly constituted by jarosite. Jarosite precipitation was more abundant when ferrous iron was initially supplemented. This precipitation negatively affected zinc bioleaching, however neither iron solubilization nor gold recovery was affected. Summarizing, the results reported in this paper suggest that the recovery of zinc as a subproduct of a biooxidation process could be possible during the biooxidation of Hualilan ore using an indigenous mesophilic consortium of iron and sulfur oxidizing-bacteria. Zinc recovery would be an extra economical support to the increase of gold recovery obtained by biooxidation process and in addition it would decrease the metallic charge of the leachates and contribute to the cleanup processes.

Acknowledgments

This work was supported by PIP 0368 from CONICET and PICT 0749 and 0623 from ANPCyT.

References

Acevedo, F., Gentina, J.C., Valencia, P., 2004. Optimization of pulp density and particle size in the biooxidation of a pyritic gold concentrate by *Sulfolobus metallicus*. World J. Microbiol. Biotechnol. 20, 865–869.

Achenbach, L., Woese, C., 1995. 16S and 23S rRNA-like primers. In: Sower, K.R., Schreier, H.J. (Eds.), Archaea: A Laboratory Manual. Cold Spring Harbor Laboratory Press, Cold Spring Harbor, NY, pp. 521–523.

Amann, R.I., 1995. In situ identification of microorganisms by whole cell hybridization with rRNA targeted nucleic acid probes. In: Akkermann, A.D.L., van Elsas, J.D., de Brujin, F.J. (Eds.), Molecular Microbial Ecology Manual. Kluwer Academic Publishers, Dordrecht, The Netherlands, pp. 1–15.

Breed, A.W., Dempers, C.J., Searby, G.E., Gardner, M.N., Rawlings, D.E., Hansford, G.S., 1999. The effect of temperature on the continuous ferrous-iron oxidation kinetics of a predominantly *Leptospirillum ferrooxidans* culture. Biotechnol. Bioeng. 65, 44–53.

Brochot, S., Durance, M.V., Villeneuve, J., d'Hugues, P., Mugabi, M., 2004. Modelling of the bioleaching of sulfide ores: application for the simulation of the bioleaching/gravity section of the Kasese Cobalt Company Ltd process plant. Miner. Eng. 17, 253–260.

Bryan, C.G., Joulian, C., Spolaore, P., El Achbouni, H., Challan-Belval, S., Morin, D., d'Hugues, P., 2011. The efficiency of indigenous and designed consortia in bioleaching stirred tank reactors. Miner. Eng. 24, 1149–1156.

Ceskova, P., Mandl, M., Helanova, S., Kasparovska, J., 2002. Kinetic studies on elemental sulfur oxidation by *Acidithiobacillus ferrooxidans*: sulfur limitation and activity of free and adsorbed bacteria. Biotechnol. Bioeng. 78, 24–30.

Chandraprabha, M.N., Modak, J.M., Natarajan, K.A., Raichur, A.M., 2002. Strategies for efficient start-up of continuous biooxidation process for refractory gold ores. Miner. Eng. 15, 751–753.

Ciftci, H., Akcil, A., 2010. Effect of biooxidation conditions on cyanide consumption and gold recovery from a refractory flotation gold concentrate. Hydrometallurgy 104, 142–149.

Curutchet, G., Donati, E., 2000. Iron-oxidizing and leaching activities of sulfur-grown *Thiobacillus ferrooxidans* cells on other substrates: effect of culture pH. J. Biosci. Bioeng. 90, 57–61.

da Silva, G., 2004. Relative importance of diffusion and reaction control during the bacterial and ferric sulphate leaching of zinc sulfide. Hydrometallurgy 73, 313–324.

Deveci, H., Akcil, A., Alp, I., 2004. Bioleaching of complex zinc sulfides using mesophilic and thermophilic bacteria: comparative importance of pH and iron. Hydrometallurgy 73, 293–303.

Dinkla, I.J.T., Gonzalez-Contreras, P., Gahan, C.S., Weijma, J., Buisman, C.J.N., Henssen, M.J.C., Sandström, Å., 2013. Quantifying microorganisms during biooxidation of arsenite and bioleaching of zinc sulfide. Miner. Eng. 48, 25–30.

Espejo, R.T., Romero, P., 1987. Growth of *Thiobacillus ferrooxidans* on elemental sulfur. Appl. Environ. Microbiol. 53, 1907–1912.

Felsenstein, J., 1985. Confidence limits on phylogenies: an approach using the bootstrap. Evolution 30, 783–791.

Fowler, T.A., Crundwell, F.K., 1999. Leaching of zinc sulfide by *Thiobacillus ferrooxidans*: bacterial oxidation of the sulfur product layer increases the rate of the sulfide dissolution at high concentrations of ferrous ions. Appl. Environ. Microbiol. 65, 5285–5292.

Ghorbani, Y., Petersen, J., Becker, M., Mainza, A.N., Franzidis, J.-P., 2013. Investigation and modelling of the progression of zinc leaching from large sphalerite ore particles. Hydrometallurgy 131–132, 8–23.

Giaveno, A., Lavalle, L., Chiacchiarini, P., Donati, E., 2007. Bioleaching of zinc from low-grade complex sulfide ores in an airlift by isolated *Leptospirillum ferrooxidans*. Hydrometallurgy 89, 117–126.

Gomez, C., Blazquez, M.L., Ballester, A., 1999. Bioleaching of a Spanish complex sulfide ore bulk concentrate. Miner. Eng. 12, 93–106.

Haghshenas, D.F., Alamdari, E.K., Bonakdarpour, B., Darvishi, D., Nasernejad, B., 2009. Kinetics of sphalerite bioleaching by *Acidithiobacillus ferrooxidans*. Hydrometallurgy 99, 202–208.

Kaewkannetra, P., Garcia-Garcia, F.J., Chiu, T.Y., 2009. Bioleaching of zinc from gold ores using *Acidithiobacillus ferrooxidans*. Int. J. Miner. Metall. Mater. 16, 368–374.

Kodali, B., Rao, B., Narasu, L., Pogaku, R., 2004. Effect of biochemical reactions in enhancement of rate of leaching. Chem. Eng. Sci. 59, 5069–5073.

Kondrat'eva, T.F., Pivovarova, T.A., Bulaev, A.G., Melamud, V.S., Muravyov, M.I., Usoltsev, A.V., Vasil'ev, E.A., 2012. Percolation bioleaching of copper and zinc and gold recovery from flotation tailings of the sulfide complex ores of the Ural region, Russia. Hydrometallurgy 111–112, 82–86.

Kupka, D., Škvarla, J., Birošová, E., 2003. Evaluation of growth rate of *Acidithiobacillus ferrooxidans* oxidizing elemental sulfur. Acta Metall. Slovaca 9, 251–258.

Levenspiel, O., 1972. Chemical Reaction Engineering. second edition. John Wiley and Sons.

Li, L., Lv, Z., Yuan, X., 2013. Effect of L-glycine on bioleaching of collophanite by *Acidithiobacillus ferrooxidans*. Int. Biodeterior. Biodegrad. 85, 156–165.

Liao, M.X., Deng, T.L., 2004. Zinc and lead extraction from complex raw sulfides by sequential bioleaching and acidic brine leach. Miner. Eng. 17, 17–22.

Lizama, H.M., 2004. A kinetic description of percolation bioleaching. Miner. Eng. 17, 23–32.

Mishra, D., Kim, D.J., Ralph, D.E., Ahn, J.G., Rhee, Y.H., 2008. Bioleaching of spent hydroprocessing catalyst using acidophilic bacteria and its kinetics aspect. J. Hazard. Mater. 152, 1082–1091.

Mousavi, S.M., Yaghmaei, S., Vossoughi, M., Jafari, A., Roostaazad, R., Turunen, I., 2007. Bacterial leaching of low-grade ZnS concentrate using indigenous mesophilic and thermophilic strains. Hydrometallurgy 85, 59–65.

Muravyov, M.I., Bulaev, A.G., 2013. Two-step oxidation of a refractory gold-bearing sulfidic concentrate and the effect of organic nutrients on its biooxidation. Miner. Eng. 45, 108–114.

Nemati, M., Harrison, S.T.L., Hansford, G.S., Webb, C., 1998. Biological oxidation of ferrous sulphate by *Thiobacillus ferrooxidans*: a review on the kinetic aspects. Biochem. Eng. J. 1, 171–190.

Rodriguez, Y., Ballester, A., Blazquez, M.L., Gonzalez, F., Munoz, J.A., 2003. New information on the sphalerite bioleaching mechanism at low and high temperature. Hydrometallurgy 71, 57–66.

Safari, V., Arzpeyma, G., Rashchi, F., Mostoufi, N., 2003. A shrinking particle—shrinking core model for leaching of a zinc ore containing silica. Int. J. Miner. Process. 93, 79–83.

Saitou, N., Nei, M., 1987. The neighbor-joining method: a new method for reconstruction of phylogenetic trees. Mol. Biol. Evol. 4, 406–425.

Shi, S.-Y., Fang, Z.-H., Ni, J.-R., 2006. Comparative study on the bioleaching of zinc sulfides. Process Biochem. 41, 438–446.

Soleimani, M., Petersen, J., Roostaazad, R., Hosseini, S., Mousavi, S.M., Najafi, A., Vasiri, A.K., 2011. Leaching of a zinc ore and concentrate using the Geocoat™ technology. Miner. Eng. 24, 64–69.

Souza, A.D., Pina, P.S., Leao, V.A., 2007. Bioleaching and chemical leaching as an integrated process in the zinc industry. Miner. Eng. 20, 591–599.

Sun, L.-X., Zhang, X., Tan, W.-S., Zhu, M.-L., 2012a. Effects of dissolved oxygen on the biooxidation process of refractory gold ores. J. Biosci. Bioeng. 114, 531–536.

Sun, L.-X., Zhang, X., Tan, W.-S., Zhu, M.-L., 2012b. Effect of agitation intensity on the biooxidation process of refractory gold ores by *Acidithiobacillus ferrooxidans*. Hydrometallurgy 127–128, 99–103.

Zhang, Y., Yang, Y., Liu, J., Qiu, G., 2013. Isolation and characterization of *Acidithiobacillus ferrooxidans* strain QXS-1 capable of unusual ferrous iron and sulfur utilization. Hydrometallurgy 136, 51–57.